Ann. Phys. (Berlin) **526**, No. 1–2, 112–117 (2014) / DOI 10.1002/andp.201300198

annalen der physik

Original Paper

Broadband efficient light absorbing in the visible regime by a metananoring array

Shuiyan Cao[1,2], *Weixing Yu*[1,*], *Lingtong Zhang*[1], *Cheng Wang*[1], *Xuming Zhang*[3], *and Yongqi Fu*[4,**]

Received 18 October 2013, accepted 18 October 2013
Published online 25 November 2013

The broadband efficient light-absorbing property of a metamaterial-based subwavelength nanoring array in visible regime is reported. The nanoring array can absorb light efficiently with an average absorptivity of 0.97 over the whole visible waveband. In addition, it is found that this kind of super light-absorbing capability is independent of the incoming light polarization state and can maintain an average of 0.9 for an incident angle as large as $\pm 60^\circ$ under TM illumination. The perfect absorbing property of the metamaterial-based nanoring array is attributed to the synergetic effect of the Fabry–Perot resonance and the localized surface plasmon resonance enhancement.

1 Introduction

Broadband light absorption in the visible regime is always interesting due to its potential applications in areas such as photodetectors, solar energy-harvesting devices, spectrum imaging sensors. Recently, various nanostructures including nanopillar, nanowire, nanocone, and nanohole arrays have been proven to have unique optical and electronic characteristics for light absorbing and harvesting [1–4]. Yang et al. reported the unique magnetic and switching characteristics of Co nanorings in the current-perpendicular-to-plane configuration [5]. In addition, Tseng et al. demonstrated the enhancing light-absorption property of a Au nanoring due to its strong localized surface plasmon resonance [6]. On the other hand, metamaterial-based structures have gained increasing interest in the last decade due to their unique extraordinary optical properties. As a result, it has been suggested as an alternative material for light absorbers [7, 8]. Recently, Cui et al. reported a one-dimensional metamaterial-based sawtooth shape absorber and it shows a good absorptive property in the mid-infrared waveband [7]. More recently, we have developed a two-dimensional pyramidal-shaped metamaterial-based absorber, which shows the surprisingly high absorptive property in an extraordinary broad waveband ranging from near-infrared to the far-infrared region [9]. Moreover, these studies mainly focused on infrared waveband and the absorptive effect of visible-light wavebands was unclear. On the other hand, the visible waveband has occupied more than 40% spectrum region of sunlight. Undoubtedly, development of the light absorber in the visible waveband is more important and profound for currently proposed low-carbon life. We report here the extraordinary light-absorbing property of a metamaterial-based nanoring array working in the visible-light waveband and the physical mechanism of the light absorbing is also explored.

2 Metananoring array

The schematic diagram of our proposed metamaterial-based nanoring array is shown in Fig. 1a. As can be seen, the nanoring array is a two-dimensional periodic structure topping a 100-nm thick Au/Si stack. There is nearly no transmission in the optical regime and light can only be absorbed or reflected by such a structure because of the existence of the alternatively layered Au thin film. The structure is designed in the subwavelength scale with 200 nm period of the nanoring in visible regime. For a single nanoring, it consists of alternating Au and Si films with thickness of $h_A = 10$ nm and

* Corresponding author E-mails: yuwx@ciomp.ac.cn
** e-mails: yqfu@uestc.edu.cn
[1] State Key Laboratory of Applied Optics, Changchun Institute of Optics, Fine Mechanics & Physics, Chinese Academy of Sciences, No.3888 South Nanhu Road, Changchun, Jilin, P. R. China
[2] University of the Chinese Academy of Sciences, Beijing, 10039, P.R. China
[3] Department of Applied Physics, Hong Kong Polytechnic University, Hung Hom, Kowloon, Hong Kong
[4] School of Physical Electronics, University of Electronic Science and Technology of China, Chengdu 610054, Sichuan Province, China

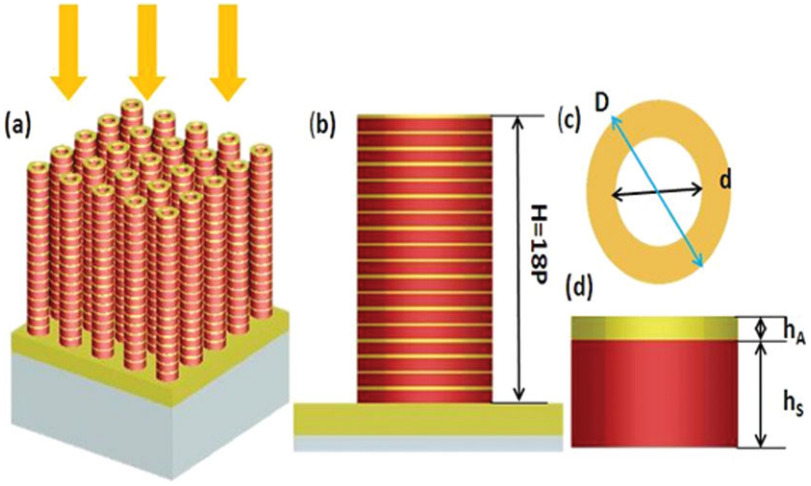

Figure 1 (a) Schematic diagram of metamaterial-based subwavelength periodic nanoring absorber; (b) Cross-sectional view of a single metananoring with Au/Si multilayer stacks; (c) Top view of a single ring; (d) Cross-sectional view of a single Au/Si stack.

$h_S = 40$ nm, as illustrated in Fig. 1d. As shown in Fig. 1c, the nanoring has an inner diameter d of 66 nm and outer diameter D of 112 nm, respectively. The total number of Au/Si pairs for each nanoring is 18.

3 Results and discussions

By means of employing finite-difference and time-domain (FDTD) methods, the absorptive spectrum of the metananoring array in visible regime was calculated, as shown in Fig. 2a. As clearly shown in the figure, the average absorptivity of the metananoring array in the whole visible waveband is as high as 0.97 and has surpassed those solar energy absorbers reported by others [1–4]. Figure 2b illustrates the absorptivity against the period of the metananoring array. The highest average absorptivity is obtained for a 200-nm period. When the period is larger than 200 nm, the absorptivity becomes worse, which is consistent with previous study and indicates that the period of a structure is smaller than the wavelength of the incident light so as to avoid scattering [10]. Figure 2c shows the effect of total number of Au/Si pairs N on absorptivity. One can see that with the increase of N, the average absorptivity becomes larger. This means the taller the metananoring, the better the absorptivity it can reach, which shows similar results as the Si nanostructure reported elsewhere before [11]. Figure 2d describes the influence of the component of Au/Si pair on absorptivity. The thickness of Au h_A is fixed at 10 nm and only the thickness of Si h_S is varied. It is found that when $h_S = 40$ nm, the absorptive effect reaches the optimum. In addition, the optimum inner and outer diameter for the metananoring is found to be 66 nm and 112 nm, respectively.

To fully characterize the absorptivity of the metananoring array, the relations between the absorptivity and the wider waveband, the polarization state as well as the incident angle of incoming light were also calculated. Figure 3a shows the absorptive spectrum in the waveband of 200 nm to 1000 nm. It is shown that although the absorptivity drops when the wavelength is larger than 700 nm, the average absorptivity in this ultra-broadband still retains a value up to 0.92. In particular, in the ultraviolet waveband, it displays extraordinary good absorptive performance. The extremely high absorptivity of the metananoring array over the ultra-broad waveband has the incomparable advantage in comparison to the pure Si nanopillar absorber that can only keep its high absorptivity in the narrow waveband ranging from 300 nm to 400 nm [11]. Figure 3b shows the absorptivity under different polarization states for 400-nm wavelength normal incident light. As shown in the figure, the absorptivity remains almost unchanged while the polarization angle changes from 0^o to 90^o. This insensitive characteristic of the absorptivity to the polarization state can be attributed to the four-fold rotational symmetry of the ring shape of the metananopillar. Figures 3c and d show the absorptive spectra at various incident angles for TM and TE wave, respectively. As can be seen from the figures, though the absorptivity drops sharply at the wavelength of 675 nm in all incident angles, the average absorptivity retains a value up to 0.9 over a wide incident angle of $\pm 60^o$ and $\pm 40^o$ for both TM and TE polarization, respectively. Such results indicate that our nanoring structure also shows a similar absorptive property as the Si nanowire does [11].

To understand the physical mechanism of the ultra-broad waveband absorptivity of the metananoring array, the energy flow distribution and y-component of

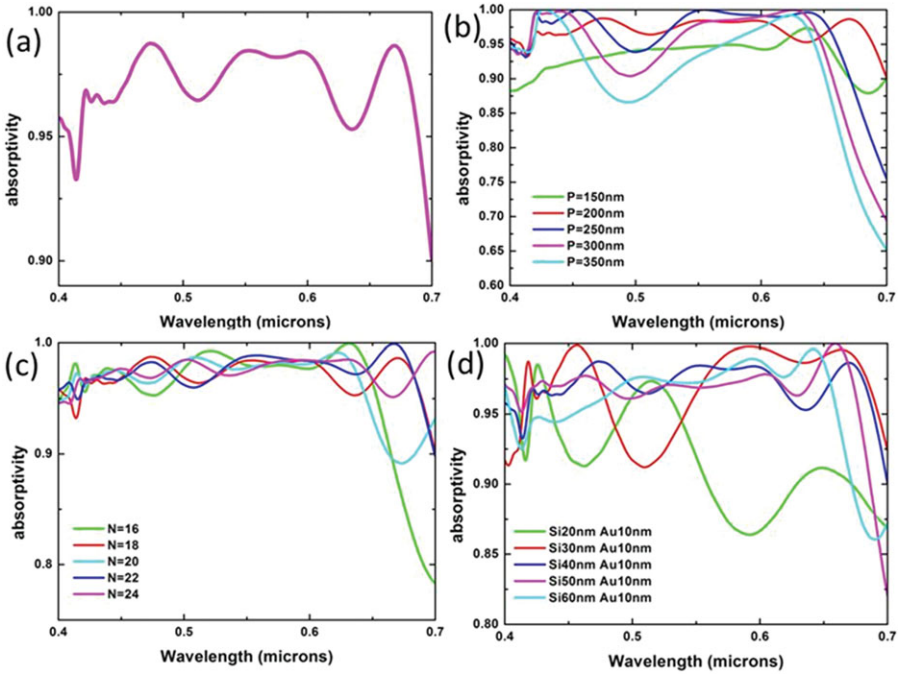

Figure 2 Absorption spectra of the metananoring array under normal incident light for various conditions. (a) under the optimal condition of $P = 200$ nm, $N = 18$, Au-10 nm/Si-40 nm, $d = 66$ nm, $D = 112$ nm; (b) for different periodicity P when $N = 18$, Au-10 nm/Si-40 nm, $d = 66$ nm, $D = 112$ nm; (c) for different total number of metal/dielectric pairs N when $P = 200$ nm, Au-10 nm-Si-40 nm, $d = 66$ nm, $D = 112$ nm; (d) for different component in a single pair when $P = 200$ nm, $N = 18$, $d = 66$ nm, and $D = 112$ nm.

the normalized magnetic-field distribution at six different wavelengths for the TM polarization were investigated and are shown in Fig. 4, where the black arrows depict the Poynting vectors **S**. Unlike the previously reported metamaterial-based saw-tooth absorber where the slow light modes are considered as the mechanism of light absorbing. However, in our case, light is mainly absorbed on the top or edge of the nanoring, which apparently, should not be attributed to the slow-light effect. It may be proposed that for the sawtooth absorber, the vortices locate exactly at the sites where the magnetic field concentrates and these are typical features in a slow-light waveguide [7]. However, in our case, although there is a concentrated magnetic field especially at longer wavelengths also, the energy flow distribution does not form vortices where there is a concentrated magnetic field. Here, we attribute the high absorptivity of the metananoring to Fabry–Perot (FP) resonance. The FP resonance model has been widely used to study the transmission through a single subwavelength slit or slit array and even the light absorption in solar cells [13, 14]. One can see clearly from Fig. 4 that FP resonance is more pronounced at longer wavelength. In particular, the FP resonance reaches a maximum at $\lambda = 680$ nm. To further elucidate the FP resonance, the absorptive spectrum for metananorings with different heights at $\lambda = 680$ nm was calculated and is shown in Fig. 5. The results clearly show that the absorptivity varies periodically as the height of metananoring increases and the period is about 250 nm. On the other hand, the effective refractive index of the metananoring was calculated to be $\mathrm{Re}(n_{\mathrm{eff}}) = 1.38$, and hence the period of the FP resonance mode (250 nm) is very close to $\lambda/(2\mathrm{Re}(n_{\mathrm{eff}})) = 246$ nm. A similar phenomenon and explanation can be found elsewhere [13].

In addition, FP resonance is not the sole mechanism for the metananoring array being used as the light absorber in which the efficient light absorption can be achieved in the whole visible regime, but is limited to those wavelengths that are close to the FP resonance wavelength. To further explore the absorptive mechanism of the metananoring array, the electric field distribution $|E_x|$ for different incident wavelengths was calculated, as shown in Fig. 6. It can be seen from Fig. 6 that the electric field hot spots are located at the side edge of the nanoring. These hot spots can be attributed to the localized surface plasmon enhancement effect. This strong local electric field intensity enhancement may be explained by the local exitation of surface palsmon polarity resonance induced by the incident light in the interface of metallic/dielectric

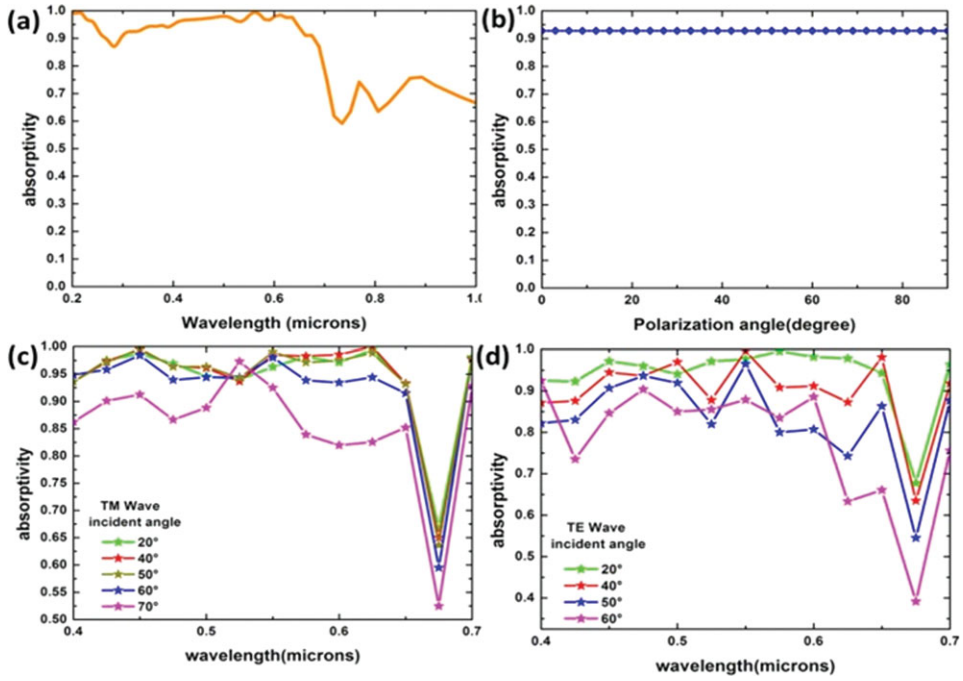

Figure 3 Absorptive spectra of metananoring array under various conditions. (a) the waveband of 200 nm to 1000 nm; (b) different polarization state when incident wavelength is 400 nm under normal incident; (c) different incident angles of 20°, 40°, 50°, 60° and 70° for a TM wave; (d) different incident angles of 20°, 40°, 50° and 60° for a TE wave.

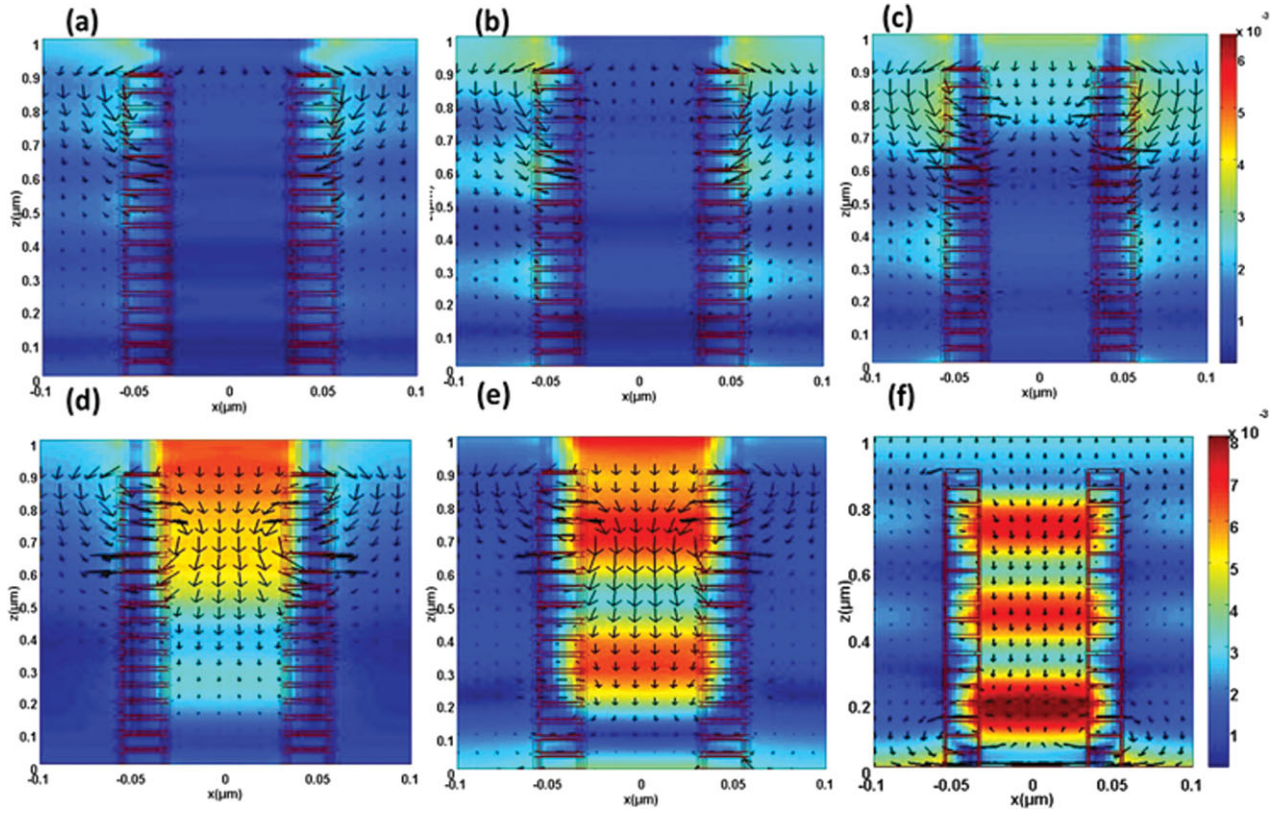

Figure 4 Distribution of magnetic field $|H_y|$ and energy flow (black arrow) for the metamaterial nanoring absorber at various wavelengths. (a) $\lambda = 400$ nm; (b) $\lambda = 480$ nm; (c) $\lambda = 550$ nm; (d) $\lambda = 600$ nm; (e) $\lambda = 650$ nm; and (f) $\lambda = 680$ nm.

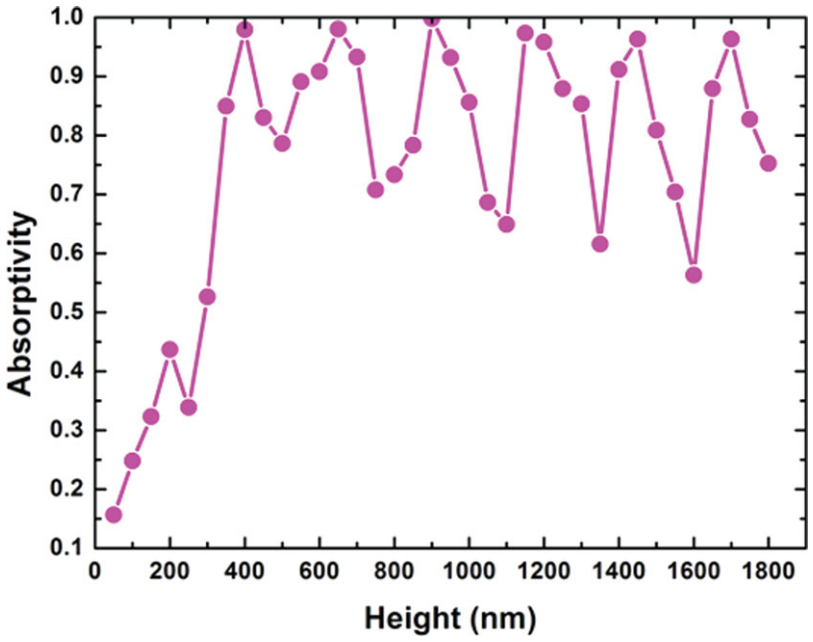

Figure 5 Absorptivity of the metananoring array with different heights under the normal incident wavelength of 680 nm.

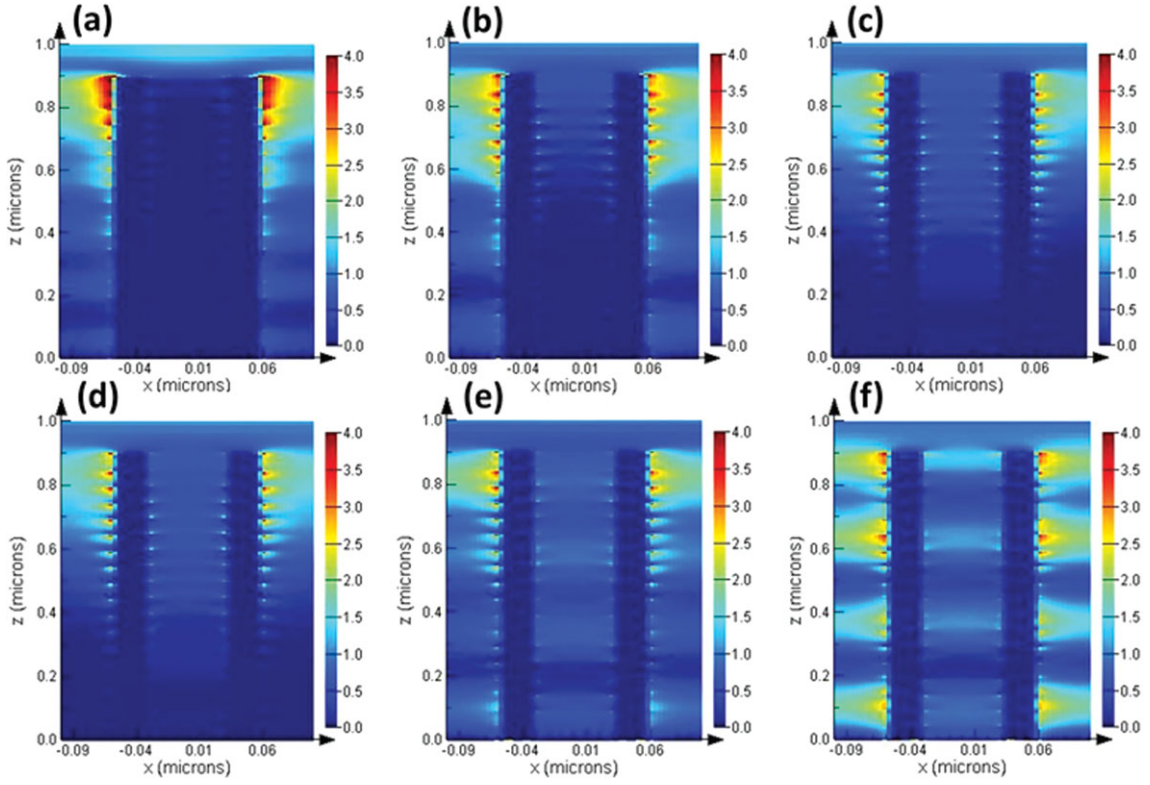

Figure 6 Electric $|E_x|$ distribution at $y = 0$ plane for different wavelengths. (a) $\lambda = 400$ nm; (b) $\lambda = 480$ nm; (c) $\lambda = 550$ nm; (d) $\lambda = 600$ nm; (e) $\lambda = 650$ nm; and (f) $\lambda = 680$ nm.

[12]. Moreover, the strong enhancement of the electric field indicates the strong charge accumulation at these sites. This can be observed from the distribution of $(|E|/|E_0|)^2$, the z-component of the electric field $(|E_z|^2)$, and the y-component of the electric field $(|E_y|^2)$ in the metal/dielectric interface, as shown in Fig. 7 (here only the plane at $z = 890$ nm and $\lambda = 680$ nm is shown as an example). It can be seen from Fig. 7 that the

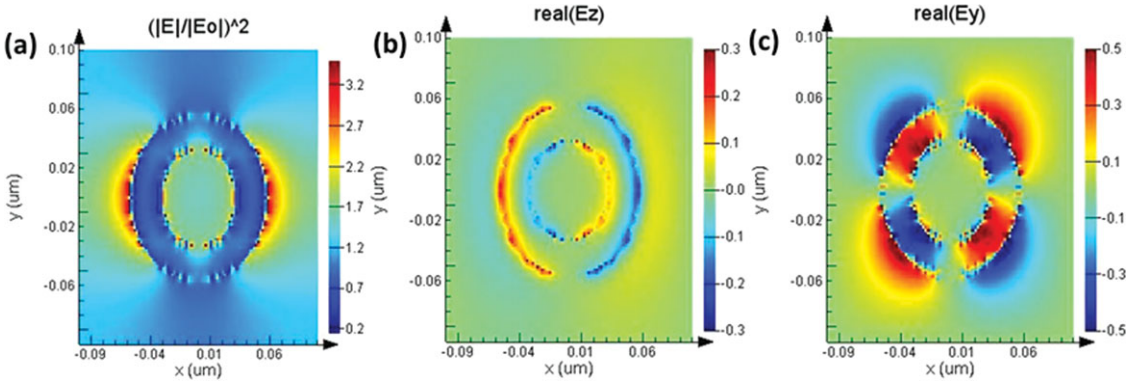

Figure 7 Distribution of (a) the electric field $(|E|/|E_0|)^2$; (b) the z-component electric field (real (E_z)); (c) the y-component electric field (real(E_y)) of the metamaterial-based nanoring absorber in the meta/dielectric interface (at $z = 890$ nm plane) at the TM wave $\lambda = 680$ nm.

opposite charges accumulating at the edges of the metal film indicate the excitation of the electric dipole resonance in the metal film [15]. The electric dipolar resonance is generated due to the localized surface plasmon resonance excited in the metal/dielectric interface and the local electric field is strong enhanced accordingly [16].

5 Conclusions

In conclusion, we have proposed a two-dimensional periodic metananoring array-based absorber that shows the efficient light-absorbing property in the whole visible regime. Our calculation results demonstrate that the absorber is insensitive to the light polarization state and able to retain the average absorptivity of 0.9 at a very large incident angle of $\pm 60^\circ$. This high light absorptivity of the metananoring array can be explained as the synergetic effect of Fabry–Perot resonance as well as localized plasmonic resonance enhancement. With the vast demand of sustainable and green energy nowadays, we believe that the proposed absorber will find its potential applications in those areas related to solar energy harvesting.

Acknowledgments. We acknowledge the financial support from the Ministry of Science and Technology of China under grant number 2010DFR10660. The financial support from the 100 Talents Program of Chinese Academy of Sciences is also acknowledged.

Key words. metaring array, broadband, visible regime, absorption.

References

[1] L. He, C. Jiang, Rusli, D. Lai, and H. Wang, Appl. Phys. Lett. **99**, 021104 (2011).
[2] O. Muskens, J. Rivas, R. Algra, E. Bakkers, and A. Lagendijk, Nano Lett. **8**, 2638–2642 (2008).
[3] J. Zhu, Z. Yu, G. Burkhard, C. Hsu, S. Connor, Y. Xu, Q. Wang, M. McGehee, S. Fan, and Y. Cui, Nano Lett. **9**, 279–282 (2009).
[4] C. Lin and M. Povinelli, Opt. Exp. **17**, 19371–19381 (2009).
[5] T. Yang, M. Hara, and A. Hirohata, Appl. Phys. Lett. **90**, 2 (2007).
[6] H.-Y. Tseng, C.-K. Lee, S.-Y. Wu, T.-T. Chi, K.-M. Yang, J.-Y. Wang, Y.-W. Kiang, C. C. Yang, M.-T. Tsai, Y.-C. Wu, H.-Y. E. Chou, and C.-P. Chiang, Nanotechnology **21**, 295102 (2010).
[7] Y. Cui, J. Xu, K. Fung, Y. Jin, A. Kumar, S. He, and X. Fang, Nano Lett. **12**, 1443–1447 (2012).
[8] Q. Liang, T. Wang, Z. Lu, Q. Sun, Y. Fu, and W. Yu, Adv. Opt. Mater. **1**, 43–49 (2013).
[9] E. M. Larsson, J. Alegret, M. Kall, and D. S. Sutherland, Nano Lett. **7**, 1256–1263 (2007).
[10] W. H. Southwell, J. Opt. Soc. Am. **A8**, 549–553 (1991).
[11] L. Hu and G. Chen, Nano Lett. **7**, 3249–3252 (2007).
[12] J. Hao, J. Wang, X. Liu, W. J. Padilla, L. Zhou, and M. Qiu, Appl. Phys. Lett. **96**, 251104 (2010).
[13] Z.-B. Li, Y.-H. Yang, X.-T. Kong, W.-Y. Zhou, and J.-G. Tian, J. Opt. A: Pure Appl. Opt. **11**, 105002 (2009).
[14] W. Wang, S. Wu, K. Reinhardt, Y. Lu, and S. Chen, Nano Lett. **10**, 2012–2018 (2010).
[15] B. X. Zhang, Y. H. Zhao, Q. Z. Hao, B. Kiraly, I. C. Khoo, S. F. Chen, and T. J. Huang, Opt. Exp. **19**, 15221 (2011).
[16] M. Pu, Q. Feng, C. Hu, and X. Luo, Plasmonics **37**, 2133–2135 (2012).